

Real-Space Manifestations of Bottlenecks in Turbulence Spectra

Uriel Frisch,¹ Samriddhi Sankar Ray,^{1,2} Ganapati Sahoo,³ Debarghya Banerjee,⁴ and Rahul Pandit^{4,*}

¹Laboratoire Lagrange, OCA, UNS, CNRS, BP 4229, 06304 Nice Cedex 4, France

²International Centre for Theoretical Sciences, Tata Institute of Fundamental Research, Bangalore 560012, India

³Max Planck Institute for Dynamics and Self-Organization, Am Fassberg 17, 37077 Göttingen, Germany

⁴Centre for Condensed Matter Theory, Department of Physics, Indian Institute of Science, Bangalore 560012, India

(Received 5 June 2012; published 4 February 2013)

An energy-spectrum bottleneck, a bump in the turbulence spectrum between the inertial and dissipation ranges, is shown to occur in the nonturbulent, one-dimensional, hyperviscous Burgers equation and found to be the Fourier-space signature of oscillations in the real-space velocity, which are explained by boundary-layer-expansion techniques. Pseudospectral simulations are used to show that such oscillations occur in velocity correlation functions in one- and three-dimensional hyperviscous hydrodynamical equations that display genuine turbulence.

DOI: [10.1103/PhysRevLett.110.064501](https://doi.org/10.1103/PhysRevLett.110.064501)

PACS numbers: 47.27.Gs, 47.10.ad

The energy spectrum $E(k)$ characterizes the statistical distribution of kinetic energy among the wave numbers k in homogeneous, isotropic, fluid turbulence in three dimensions (3D). If k_I and k_d denote, respectively, the wave vector magnitudes related to the inverses of the lengths L_I , at which energy is injected into the system, and η_d , where viscous dissipation becomes significant, then, in the inertial range $k_I \ll k \ll k_d$, this spectrum scales as $E(k) \propto k^{-n}$; the phenomenological theory (K41) of Kolmogorov [1], which does not account for intermittency [2], yields $n = 5/3$ for 3D fluid turbulence. In the far-dissipation range $k \gg k_d$, this spectrum falls off exponentially (up to algebraic prefactors) [3]. For values of k between inertial and far-dissipation ranges, a plot of the *compensated* energy spectrum $[k^n E(k)]$ versus k exhibits a gentle maximum that is called a *bottleneck* [4,5]. Such bottlenecks have been seen in a variety of experiments [6,7] and in direct numerical simulations (DNSs) of fluid turbulence [7–10]. Phenomenological mechanisms have been suggested for the formation of bottlenecks (see, e.g., Refs. [4,5]). A systematic theoretical study of the bottleneck phenomenon has been initiated in Ref. [11] by using the limit of high dissipativity α in hyperviscous hydrodynamical equations, which have a dissipation operator $\propto (-\nabla^2)^\alpha$. Hyperviscous dissipation, with moderate values of α , e.g., 2 and 4, is often used in DNSs in the hope of enhancing the inertial range, but at the price of producing increasingly strong bottlenecks [11].

In the first part of our study we develop a quantitative, analytical understanding of bottlenecks in the following hyperviscous generalization of the one-dimensional Burgers equation:

$$\partial_t u + u \partial_x u = -\nu_\alpha k_r^{-2\alpha} (-\partial_x^2)^\alpha u + f(x, t). \quad (1)$$

Here, $u(x, t)$ is the velocity at the point x and time t , $\nu_\alpha > 0$ the hyperviscosity, k_r a reference wave number, and f the driving force. It is well known that the ordinary ($\alpha = 1$)

Burgers equation, with $f = 0$, is integrable [12]; it is also easy to show that its energy spectrum has no bottleneck. By contrast, we show that, for any integer $\alpha > 1$, the solution to the hyperviscous Burgers equation (1), in the limit of small ν_α , displays an energy-spectrum bottleneck; for this it is crucial to examine the solution in real space, where we can use boundary-layer-type analysis, in the vicinities of shocks, to uncover oscillations in the velocity profile. We obtain this result for both the unforced, hyperviscous Burgers equation and for its variant (DHB) with deterministic, time-independent, large-scale forcing. We validate our DHB solutions with a pseudospectral DNS. Note that these solutions are time independent and not turbulent; however, the key qualitative feature of real-space oscillations in the velocity profile does carry over to oscillations in velocity correlation functions in one- and three-dimensional hyperviscous hydrodynamical equations that display genuine turbulence. We show this in the second part of our study by using DNS. This association of bottlenecks and oscillations in velocity correlation functions has not been made so far. It is akin to the association of peaks in the static structure factor $S(k)$, of a liquid in equilibrium, with damped oscillations in the radial distribution function $g(r)$ [13].

The simplest model presented here, which displays a bottleneck amenable to analytical study, is the DHB equation (1) with integer $\alpha > 1$, time-independent force $f = \sin x$, and $u(x, t = 0) = 0$. The velocity eventually goes to a steady state, which is a solution of the ordinary differential equation (ODE) that is obtained by dropping the time-derivative term in (1). When $\alpha \neq 1$, this nonlinear ODE is not integrable, but its limit as $\nu_\alpha \rightarrow 0$ is the same as for ordinary dissipation; namely, it has a shock at $x = \pi$, where the solution jumps from $u_- = +2$ to $u_+ = -2$. For small but finite ν_α , the shock is broadened and its structure can be analyzed by a boundary-layer technique using the stretched spatial variable $X \equiv (x - \pi)/\nu^\beta$, with

$\beta = \frac{1}{2\alpha-1}$, and expanding the boundary-layer velocity u^{BL} in powers of ν_α : $u^{\text{BL}}(X) = \sum_{j=0}^{\infty} \nu_\alpha^j u_j(X)$. To leading order ($j = 0$)

$$\frac{d}{dX} \left(\frac{u_0^2}{2} \right) = (-1)^{\alpha+1} \frac{d^{2\alpha}}{dX^{2\alpha}} u_0, \quad u_0(\pm\infty) = \mp 2. \quad (2)$$

For $\alpha = 1$, we obtain the standard profile $u_0 = -2 \tanh X$. For $\alpha > 1$, Eq. (2) cannot be solved analytically. However, for large X the equation can be linearized because u_0 is close to its asymptotic constant value. For example, for large negative X , we set $u_0 = 2 + w$, discard the quadratic term in w , and obtain, after integrating once, $(-1)^{\alpha+1} d^{2\alpha-1} w / dX^{2\alpha-1} = 2w$. This constant-coefficient ODE has solutions of the form $\mu \exp(\kappa_\alpha X)$, where μ is arbitrary and the ‘‘eigenvalue’’ κ_α is any of the $(2\alpha - 1)^{\text{th}}$ roots of $(-1)^{\alpha+1} 2$; i.e., for even α , $\kappa_\alpha = 2^\beta \exp[i(2n + 1)\beta\pi]$ and for odd α , $\kappa_\alpha = 2^\beta \exp(i2n\beta\pi)$, with $n = 0, 1, \dots, (2\alpha - 2)$. Only the eigenvalues that have a positive real part are acceptable because w should vanish at $-\infty$. If all the modes with such eigenvalues are actually present then, for $X \rightarrow -\infty$, the solution to (2) tends to $+2$ in an *oscillatory* fashion and it is dominated by the mode n_* (and its complex conjugate), which has the smallest positive real part. In terms of the unstretched coordinates, this means that, in the neighborhood of the shock, the solution for even α displays damped oscillations with wavelength

$$\lambda_\alpha^{\text{th}} = 2\pi \nu_\alpha^\beta \{2^\beta \sin[(2n_* + 1)\beta\pi]\}^{-1} \quad (3)$$

and with an e -folding rate

$$K_\alpha^{\text{th}} = 2^\beta \nu_\alpha^{-\beta} \cos[(2n_* + 1)\beta\pi]. \quad (4)$$

The case of odd α is handled *mutatis mutandis*.

Such damped oscillations imply the presence of a pair of complex k poles in wave number space, whose signature, for real k , is a Lorentzian. This can be a bump or a trough, near wave number $2\pi/\lambda_\alpha$, with width $\sim K_\alpha$ and amplitude $\sim K_\alpha^{-1}$. We present below a seminumerical analysis to show that the solution of the DHB yields a bottleneck (bump).

The theory presented here can be applied to a wide class of problems ranging from the unforced, hyperviscous Burgers equation to the case of arbitrary, large-scale, time-dependent or time-independent forcing as long as it does not modify the internal structure of shocks. Note also that such a linearized theory gives no prediction for the α dependence of the amplitude of the bottleneck. Furthermore, when more than one mode (or pair of complex-conjugate modes) with a positive real part is present (i.e., for $\alpha \geq 3$), linear theory does not tell us if the mode(s) with the smallest positive real part is (are) actually excited. Such issues require a global analysis of the boundary-layer equation (2) and not just of its large- X , linearized version. Except for the very standard case of

ordinary dissipation, we do not know much about the properties of the solution to Eq. (2). If we demand that $u_0(X=0) = 0$ (which can always be achieved by a suitable translation), is the solution unique? By using a numerical, shooting method, we obtain evidence that, for $\alpha = 2$, there is a unique solution that has $u_0'(X)|_{X=0} = -2.121530817618\dots$ and $u_0''(X)|_{X=0} = 0$. We can also obtain the value of this first derivative at the origin with $\approx 10\%$ accuracy by assuming that the solution has singularities on the imaginary axis at $X = Z_* = \pm i\Delta$ [a Painlevé-type argument indicates that, near such a singularity, to leading order, $u_0(X) \approx 120/(X - Z_*)$]. The vanishing of the second derivative implies that this unique solution is odd.

Direct numerical integration of the boundary-layer equation (2) is a greater challenge than the full DHB equation because, for the latter, we can take advantage of periodic boundary conditions. By using the value of $u_0'(0)$ and $u_0''(0) = 0$, we solve the third-order, boundary-layer equation for $\alpha = 2$ numerically. We find $X_C \approx 1.15$, the value of X at which $u_0(X)$ first crosses the -2 asymptote. Next, we calculate $u_0'(X_C)$ by using the Taylor expansion $u_0(X) \sim u_0'(0)X + u_0'''(0)X^3/3! + u_0''''(0)X^5/5! + \dots$ along with the known values of u_0' and $u_0''(0) = 2$ and $u_0''''(0) = -(u_0'(0))^2$ [from Eq. (2)]. The linear theory suggests $u_0(X) = -2 + A e^{-K_2(X-X_C)} \sin 2\pi(X - X_C)/\lambda_2$ for $X \geq X_C$; hence, we obtain $u_0'(X_C)$ in terms of A and λ_2 . By using the values of $u_0'(X_C)$ and λ_2 [cf. Eq. (3)], we obtain $A \approx -0.983$, which is within 1.7% of the value of A (≈ -0.966) that we get from the solution of the boundary-layer equation.

We now address the question of whether the Fourier-space manifestation of these oscillations is a bump or a trough. The Fourier transform $\gamma(k)$ of the real and even function $-u'(X)$ is real and even [14], and $\gamma(k)$ is the square root of the compensated energy spectrum. The rising of the compensated energy spectrum between the flat region near $k = 0$ and the exponential decay at large k is equivalent to $\gamma''(k)$ being positive, and $\gamma''(k)|_{k \rightarrow 0} = 1/2\pi \int_0^\infty dX X^2 u'(X)$. To solve for $\gamma''(k)$, we use $u'(X)$ either from a numerical solution of Eq. (2) or from the linear theory; we then perform a numerical integration over X , we obtain reasonable agreement ($\approx 9\%$) between the results of both these methods, and, indeed, we find that $\gamma''(k)$ is positive, so the spectrum has a bottleneck.

We turn now to a pseudospectral DNS of the DHB equation (1) with $\alpha = 2, 4, 8$, and 16, a 2/3 rule for dealiasing, and a fourth-order, Runge-Kutta method for time integration. The reference wave number $k_r = 100$, the number of collocation points $N = 2^{14}$, the time step $\delta t = 10^{-4}$, and the hyperviscosity coefficients are $\nu_2 = 5 \times 10^{-3}$, $\nu_4 = 5 \times 10^{-8}$, $\nu_8 = 5 \times 10^{-14}$, and $\nu_{16} = 10^{-20}$.

The steady-state, compensated energy spectra $E_k^c \equiv k^2 E(k)$ [Fig. 1(a)] show clear bottlenecks; the height of

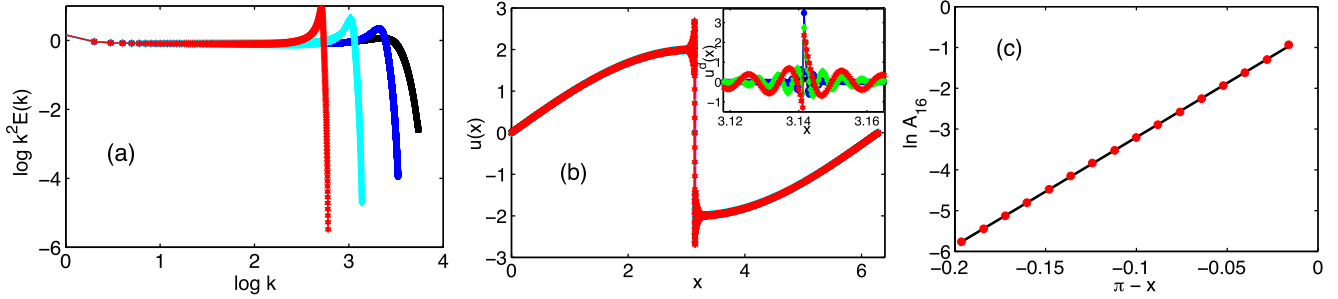


FIG. 1 (color online). Plots for the DHB Eq. (1). (a) Log-log plots of the compensated energy spectrum $k^2 E(k)$ versus k for $\alpha = 2$ (black squares), $\alpha = 4$ (blue filled-circles), $\alpha = 8$ (green diamonds), and $\alpha = 16$ (red hexagons). (b) Plots of the steady-state solution $u(x)$ for the same values of α as in (a); these are indistinguishable from $u^o(x)$ (thick magenta line) away from $x = \pi$. Inset: Plots of $u^d(x)$ versus x around $x = \pi$. (c) Semilog plot of A_{16} (red filled circles) versus $\pi - x$; the black line is the fit.

the bottleneck peak increases with α , but k_b^α , the wave number of this peak, decreases as we increase α . We now investigate the real-space manifestation of this bottleneck. In Fig. 1(b) we plot the steady-state solution of the DHB equation; this shows that our numerical solution agrees with the *outer* solution $u^o(x) = 2\text{sgn}(\pi - x)\sin(x/2)$ away from the shock. However, in a thin boundary layer around the shock at $x = \pi$, there are oscillations that become prominent when we plot the difference between the solution of the DHB equation and the outer solution, $u^d(x) \equiv u(x) - u^o(x)$, versus x [Fig. 1(b), inset]. The characteristic wavelength of these oscillations is λ_α ; for the representative case $\alpha = 16$, we find $\lambda_{16} = 0.0122$. Similarly, from plots of the compensated spectra [Fig. 1(a)] we obtain $\lambda_{16} = 0.0121$. Furthermore, the theoretical prediction for the wavelength of these oscillations [cf. Eq. (3)] yields $\lambda_{16}^{\text{th}} = 0.0120$. The bottleneck has a finite width because of the decaying envelope of the oscillations as we move away from the shock [cf. Eq. (4)]. We obtain the amplitude A_α of these oscillations [Fig. 1(b)] as a function of $(x - \pi)$ and find, numerically, that $A_\alpha \sim \exp[K_\alpha(x - \pi)]$ as shown in Fig. 1(c). For $\alpha = 16$ we obtain, from our DNS, an e -folding rate $K_{16} \approx 26.61$, whereas our theoretical prediction in Eq. (4) yields $K_{16}^{\text{th}} \approx 26.54$. Thus, we find excellent agreement between our

theoretical predictions [Eqs. (3) and (4)] and our numerical results for both the wavelength of the oscillations and the e -folding rate.

We now provide numerical evidence of the presence of small oscillations, in the velocity correlation functions, in the stochastically forced hyperviscous Burgers equation (SHB) and the 3D hyperviscous Navier-Stokes (HNS) equations, both of which exhibit turbulence. Let us first examine bottlenecks in the SHB equation [15], with a white-in-time, Gaussian random force with zero mean, an ultraviolet cutoff at $N/8$, and a spectrum $\sim k^{-1}$. The velocity field for the SHB shows shocks at various length scales, and the resulting energy spectrum shows an inertial-range scaling $E(k) \sim k^{-5/3}$. In Fig. 2(a) we give a representative plot of the compensated energy spectrum $k^{5/3}E(k)$, for $\alpha = 8$; this shows a prominent bottleneck that peaks at a wave number $k_b^8 \approx 890$. We measure the correlation function $D_{\text{SHB}} = \langle u(x)u(x+r) \rangle / \langle u(x)^2 \rangle$, which shows oscillations that are the real-space manifestations of the bottleneck. These oscillations are best seen in a plot of D_{SHB}^o , which is D_{SHB} with the decaying trend subtracted out [Fig. 2(a), inset]. The wavelength of these oscillations is ≈ 0.00706 , and the corresponding wave number is ≈ 889.97 , in agreement with the wave number of the bottleneck peak in Fig. 2(a).

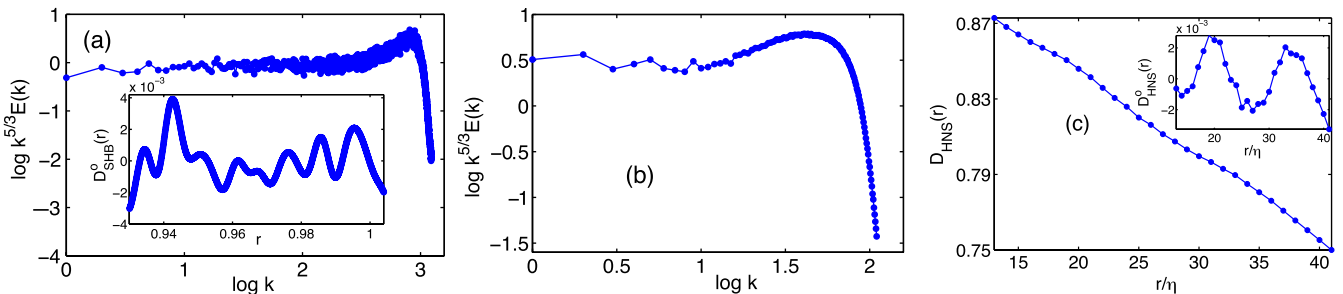


FIG. 2 (color online). (a) Log-log plot of the compensated energy spectrum $k^{5/3}E(k)$ versus k for the SHB equation with $\alpha = 8$ and (inset) a plot of its correlation function D_{SHB}^o showing oscillations of wavelength λ_8^{SHB} , which is inversely related to the wave number of the bottleneck. (b) The compensated energy spectrum $k^{5/3}E(k)$ for the 3D HNS equation ($\alpha = 4$) with a bottleneck peak at wave number $K_{b,\alpha}^{\text{HNS}} = 40$. (c) A plot of the correlation function $D_{\text{HNS}}(r)$ versus r/η , where η is the Kolmogorov scale [16], for the 3D HNS equation. Inset: Oscillations in a plot of the function $D_{\text{HNS}}^o(r)$.

The 3D HNS equation for an incompressible velocity field $\mathbf{u}(\mathbf{x}, t)$ is

$$\frac{\partial \mathbf{u}}{\partial t} + \mathbf{u} \cdot \nabla \mathbf{u}(\mathbf{x}, t) = -\nabla p - \nu_\alpha (-\nabla^2)^\alpha \mathbf{u}(\mathbf{x}, t) + \mathbf{f}(\mathbf{x}, t);$$

$$\nabla \cdot \mathbf{u} = 0. \quad (5)$$

We integrate it by a pseudospectral method with a 2/3 dealiasing rule, an Adams-Bashforth scheme for time marching, 512^3 collocation points, $\alpha = 4$, and $\nu_4 = 10^{-14}$. We force the 3D HNS equation to a statistically steady state by using a constant-energy-injection method [16]. In Fig. 2(b), we show a representative plot of the compensated energy spectrum $E^c(k) \equiv k^{5/3} E(k)$; this shows a bottleneck between the inertial and dissipation ranges. The full correlation function $D_{\text{HNS}}(r) = \langle \mathbf{u}(\mathbf{x}) \cdot \mathbf{u}(\mathbf{x} + \mathbf{r}) \rangle / \langle u_{\text{rms}}^2 \rangle$, averaged over five configurations that are separated from each other by $6\tau_I$, where τ_I is the integral-scale eddy turnover time and u_{rms} is the root-mean-square velocity from our DNS, shows gentle oscillations [Fig. 2(c)], which are the real-space manifestations of this bottleneck. These oscillations can be seen clearly in $D_{\text{HNS}}^o(r)$ [Fig. 2(c), inset], which is obtained by subtracting the decaying trend from $D_{\text{HNS}}(r)$. The wavelength of these oscillations is $\simeq 0.1665$ and the corresponding wave number is $\simeq 37.7$, in agreement with the wave number at which the bottleneck shows a peak in Fig. 2(b). We note that these oscillations are weak and localized between the inertial and dissipation ranges, so it is unlikely that they substantially affect calculations of inertial-range multiscaling exponents of structure functions by standard techniques, such as local-slope analyses, are unlikely to be affected substantially. Technically, we are trying to capture subdominant contributions of the oscillations to the structure functions by looking at leading-order behaviors. However, recent work on improved simulation data processing (by using high-precision simulations) indicates that ignoring such subdominant corrections leads to poor accuracy in determining leading-order exponents [17]. Similarly, the very tiny discrepancies between longitudinal and transverse scaling exponents, which are sometimes reported [18], may not be resolved until we use better processing techniques, for these could just be discrepancies in subdominant terms.

We have provided a theoretical explanation for energy-spectra bottlenecks in the DHB equation by combining analytical and numerical studies. These bottlenecks appear as a natural consequence of oscillations in the velocity profiles in the vicinity of a shock. Earlier studies [19,20] have seen such oscillations in the DHB case but have not associated them with bottlenecks. Furthermore, we have shown that bottlenecks in the SHB and the 3D HNS equations, which exhibit turbulence, are associated with damped oscillations in real-space velocity correlation functions. This association has not been made hitherto, even though there have been attempts to explore real-space

manifestations of bottlenecks. This is the signature that Donzis and Sreenivasan were looking for in Ref. [10]. Our work confirms that the larger the dissipativity α , the more pronounced the bottleneck [7,11,21]. Energy spectra for homogeneous isotropic turbulence in the 3D NS equation ($\alpha = 1$) show a mild bottleneck [9,11]; we expect, therefore, that there should be weak oscillations in real-space velocity correlation functions, whose detection is an important challenge for experiments and DNS.

We address, briefly, the delicate issue of the interplay between intermittency and bottlenecks. Intermittency implies, among other things, that the inertial-range energy spectrum $E(k)$ has a correction to the K41 scaling. This correction is proportional to $(k/k_0)^{-\delta}$, where k_0 is the wave number associated with the integral scale and δ is a small positive number. The solution to the standard Burgers equation, where δ is $1/3$, constitutes an extreme form of intermittency, in which all small-scale activity is concentrated in the shocks. In the presence of ordinary viscous dissipation, in the Burgers equation, it is tempting to ask if it is this intermittency that prevents the bottleneck. It is useful here to consider the very opposite case of problems that have no intermittency, e.g., the K41-compatible closure models like the Eddy-Damped-Quasi-Normal-Markovian (EDQNM) approximation [22], which have no intermittency but do display bottlenecks (see Fig. 1 in Ref. [11]). For such closures it might be possible to understand the bottleneck as a consequence of positive, subdominant contributions, which make the compensated spectrum rise slowly before it drops in the far-dissipation range. For realistic models of turbulence, which do include intermittency, the correction to K41 scaling arising from intermittency ($-\delta$) is negative, and it may, therefore, mask or suppress the bottleneck. Furthermore, intermittency corrections involve terms which depend on k/k_0 , whereas the subdominant corrections involve k/k_d and, except in the case of the Burgers equation, we do not have a strong analytical understanding of intermittency. Hence, at this stage it is difficult to come to any definite conclusion about whether bottlenecks do go away as the Reynolds number goes to infinity as conjectured in Ref. [10].

We thank W. Pauls, K. R. Sreenivasan, and A. Wirth for discussions, CSIR, UGC, and DST (India) for support, and SERC (IISc) for computational resources. U. F. and R. P. are members of the International Collaboration for Turbulence Research; U. F., R. P., and S. S. R. acknowledge support from the COST Action MP0806; the work of U. F. and S. S. R. was supported by ANR ‘‘OTARIE’’ BLAN07-2_183172; S. S. R. also thanks the European Research Council under the European Community’s Seventh Framework Program (FP7/2007-2013, Grant Agreement No. 240579) for support; D. B. and R. P. thank the Observatoire de la Côte d’Azur for hospitality; and U. F. thanks the Indian Institute of Science for the DST-IISc Centenary Professorship.

- *Also at: Jawaharlal Nehru Centre for Advanced Scientific Research, Jakkur, Bangalore, India.
- [1] A. N. Kolmogorov, Dokl. Akad. Nauk SSSR **30**, 299 (1941); A. N. Kolmogorov, Proc. R. Soc. A **434**, 9 (1991).
- [2] U. Frisch, *Turbulence: The Legacy of A. N. Kolmogorov* (Cambridge University Press, Cambridge, England, 1995).
- [3] J. von Neumann, in *Collected Works (1949-1963)*, edited by A. H. Taub (Pergamon, New York, 1963), Vol. 6, pp. 37–472. As first observed by von Neumann, this follows from the (conjectured) analyticity of the solution of the Navier-Stokes equation.
- [4] G. Falkovich, Phys. Fluids **6**, 1411 (1994).
- [5] D. Lohse and A. Müller-Groeling, Phys. Rev. Lett. **74**, 1747 (1995).
- [6] H. K. Pak, W. I. Goldburg, and A. Sirivat, Fluid Dyn. Res. **8**, 19 (1991); Z.-S. She and E. Jackson, Phys. Fluids A **5**, 1526 (1993); S. G. Saddoughi and S. V. Veeravalli, J. Fluid Mech. **268**, 333 (1994).
- [7] W. Dobler, N. E. L. Haugen, T. A. Yousef, and A. Brandenburg, Phys. Rev. E **68**, 026304 (2003).
- [8] Z.-S. She, S. Chen, G. Doolen, R. H. Kraichnan, and S. A. Orszag, Phys. Rev. Lett. **70**, 3251 (1993); P. K. Yeung and Y. Zhou, Phys. Rev. E **56**, 1746 (1997); T. Gotoh, D. Fukayama, and T. Nakano, Phys. Fluids **14**, 1065 (2002); M. K. Verma and D. A. Donzis, J. Phys. A **40**, 4401 (2007); P. D. Mininni, A. Alexakis, and A. Pouquet, Phys. Rev. E **77**, 036306 (2008).
- [9] Y. Kaneda, T. Ishihara, M. Yokokawa, K. Itakura, and A. Uno, Phys. Fluids **15**, L21 (2003); T. Ishihara, T. Gotoh, and Y. Kaneda, Annu. Rev. Fluid Mech. **41**, 165 (2009); S. Kurien, M. A. Taylor, and T. Matsumoto, Phys. Rev. E **69**, 066313 (2004).
- [10] D. A. Donzis and K. R. Sreenivasan, J. Fluid Mech. **657**, 171 (2010).
- [11] U. Frisch, S. Kurien, R. Pandit, W. Pauls, S. S. Ray, A. Wirth, and J.-Z. Zhu, Phys. Rev. Lett. **101**, 144501 (2008).
- [12] J. Bec and K. Khanin, Phys. Rep. **447**, 1 (2007).
- [13] See, e.g., J.-P. Hansen and I. R. McDonald, *Theory of Simple Liquids* (Academic, London, 2006); J. L. Yarnell, M. J. Katz, R. G. Wenzel, and S. H. Koenig, Phys. Rev. A **7**, 2130 (1973).
- [14] This can be checked numerically. Also, because $-u'(0) > 0$ and we are within the radius of convergence of the Taylor expansion of $u(X)$, as obtained from the Painlevé-type analysis, $\gamma(k)$ cannot suddenly become negative without being positive for at least some small region.
- [15] D. Mitra, J. Bec, R. Pandit, and U. Frisch, Phys. Rev. Lett. **94**, 194501 (2005).
- [16] A. G. Lamorgese, D. A. Caughey, and S. B. Pope, Phys. Fluids **17**, 015106 (2005).
- [17] J. van der Hoeven, J. Symb. Comput. **44**, 1000 (2009); W. Pauls and U. Frisch, J. Stat. Phys. **127**, 1095 (2007); S. Chakraborty, U. Frisch, W. Pauls, and S. S. Ray, Phys. Rev. E **85**, 015301(R) (2012).
- [18] L. Biferale and I. Procaccia, Phys. Rep. **414**, 43 (2005); T. Ishihara, T. Gotoh, and Y. Kaneda, Annu. Rev. Fluid Mech. **41**, 165 (2009), and references therein.
- [19] J. P. Boyd, J. Atmos. Sci., **49**, 128 (1992); J. Sci. Comput. **9**, 81 (1994).
- [20] W. Pauls and J. Zudrop (unpublished).
- [21] D. Biskamp, E. Schwarz, and A. Celani, Phys. Rev. Lett. **81**, 4855 (1998); D. Biskamp and W.-C. Müller, Phys. Plasmas **7**, 4889 (2000).
- [22] S. A. Orszag, in *Fluid Dynamics*, Proceedings of the Les Houches Summer School, Session 1973, edited by R. Balian and J. L. Peube (Gordon and Breach, New York, 1977), p. 273.